



Experimental investigation and modeling of date drying under forced convection solar dryers

T. Seerangurayar^{1,2} · Abdulrahim M. Al-Ismaili¹ · L. H. Janitha Jeewantha³ · G. Jeevarathinam² · R. Pandiselvam⁴ · S. Dinesh Kumar² · M. Mohanraj² · Punit Singh⁵

Received: 11 February 2023 / Revised: 24 May 2023 / Accepted: 2 June 2023 / Published online: 16 June 2023
© The Author(s), under exclusive licence to Springer-Verlag GmbH Germany, part of Springer Nature 2023

Abstract

This paper presents the drying behavior of fresh dates at three ripeness stages (khalal, rutab, and tamr) in three drying techniques, namely, direct sun drying (DSD), greenhouse-like solar drying (GSD), and indirect convective solar drying (ISD) and validated with drying models. The experimental data was fitted to 11 thin-layer drying models to identify the best model to describe the drying behavior of the dates in the three solar drying methods. The results showed that using DSD, the safe moisture level of 35% on dry basis was reached in 86 h for khalal, 103 h for rutab, and 103 h for tamr. However, GSD has the faster drying rate, reaching the final moisture content in 53 h for khalal, 64 h for rutab, and 61 h for tamr, compared to 75 h, 70 h, and 70 h in ISD for the respective stages of ripeness. The Midilli and Kucuk, Diffusion approach, Logarithmic, Two-term, and Verma models were found to be the most suitable for representing the drying process of fresh dates.

Keywords Dates drying · Direct sun drying · Greenhouse-like solar dryer · Indirect convective solar dryer · Drying characteristics

Nomenclature

$p, q, g, n, k, k_0,$ and k_1 Empirical constants in drying models
 N Number of observations

M Number of constants in a model
 T Time (s, min, h)
 M_w Moisture content of the dates after harvest in wet basis
 M_d Moisture content of the dates after harvest in dry basis
 M_o Initial moisture content (kg water/kg dry matter)
 M_e Equilibrium moisture content (kg water/kg dry matter)
 M_t Moisture content at any given time (kg water/kg dry matter)
 W_i Initial weight (kg)
 W_d Oven-dried weight (kg)
 W_t Weight of the product at any given time (kg)
 DR Drying rate (kg/h)
 MR Moisture ratio (dimensionless)
 $MR_{exp,i}$ i^{th} experimental value of the moisture ratio
 $MR_{pre,i}$ i^{th} predicted value of the moisture ratio
 \overline{MR}_{pre} Average predicted value of the moisture ratio
 R^2 Coefficient of determination

✉ T. Seerangurayar
rayar.tnau@gmail.com

✉ G. Jeevarathinam
jeevaganesan.tnau@gmail.com

✉ R. Pandiselvam
anbupandi006@gmail.com; r.pandiselvam@icar.gov.in

¹ Department of Soils, Water and Agricultural Engineering, College of Agricultural and Marine Sciences, Sultan Qaboos University, Al-Khoud 123, Muscat, Oman

² Hindusthan College of Engineering and Technology, Coimbatore 641 032, Tamil Nadu, India

³ Centre for Future Materials & School of Mechanical and Electrical Engineering, Faculty of Health Engineering and Sciences, University of Southern Queensland, Toowoomba, QLD, Australia

⁴ Physiology, Biochemistry and Post-Harvest Technology Division, ICAR–Central Plantation Crops Research Institute, Kasaragod 671 124, Kerala, India

⁵ Department of Mechanical Engineering, Institute of Engineering and Technology, GLA University Mathura, Uttar Pradesh, Chaumuhan 281406, India

Abbreviations

| | |
|------|---------------------------------|
| DSD | Direct sun drying |
| GSD | Greenhouse-like solar dryer |
| ISD | Indirect convective solar dryer |
| RMSE | Root mean square error |
| DB | Dry basis (moisture content) |
| WB | Wet basis (moisture content) |
| RH | Relative humidity |

Greek symbols

| | |
|----------|----------------------|
| χ^2 | Chi-square (reduced) |
|----------|----------------------|

Subscript

| | |
|-----|-------------------|
| 0 | Initial |
| e | Equilibrium |
| t | At any given time |

1 Introduction

In the MENA (Middle East and North Africa) region, date palm trees (*Phoenix dactylifera*. L) are considered one of the oldest, most important, and principal crop. It is vital in the socioeconomic, cultural, and environmental activities of the people in these areas [1]. Oman is a major date producer where date palm covers 35% of the total cultivated area and 78% of all fruit crops grown. The available date palm trees in Oman is 7.6 millions and cultivated in 24,120 ha [2]. In 2013, Oman date production was 308,400 tons but it exported only 8992 tons (2.9% of total production). In the same year, about 9129 tons of dates was imported [3]. The export quantity of date is always lower than the import quantity in Oman which could be attributed to poor handling, fruit quality, and postharvest methods adopted. Therefore, developing new postharvest techniques is very essential for sustainable cultivation of dates in Oman.

Drying is one among the oldest postharvest techniques mainly to protect the high-moisture foods from spoilage and also enhances the postharvest life [4]. Fresh dates are mostly consumed when they are half-ripe (rutab stage) but some varieties are preferably consumed after they get mature (khalal stage) or when they are full-ripe (tamr stage) [5]. Commercially available dates are fresh, dried, and processed dates [6]. Fresh dates are commonly dried in open or direct sun drying due to its simplicity and cost effectiveness [7]. However, the dried dates produced in this method are having poor quality due to the influence of dust and sand particles and can be exposed to birds and insects [8, 9]. In addition, direct exposure to sun might cause date hardening in the sunny days, which may lead to poor quality products.

Solar dryer can overcome the limitations associated with direct sun drying [10, 11]. They could be a useful device to dry a large quantity of foodstuffs by reducing drying time in less area with cost effectiveness [12]. The solar dryers are

the most attractive and promising for dehydration of agriculture materials [10, 13]. Several studies proved that solar dryers are the successful alternative to direct sun drying as they produce good quality dried products such as tomato [14], strawberry [15], plum [16], red chili [10, 13], turmeric [17], and black turmeric [18].

Drying rate is influenced by three main factors, viz., air temperature, moisture, and air speed. From thermodynamic viewpoint, the drying rate is nonlinear as the transfer of heat and moisture from the products takes place simultaneously but unsteadily [19]. Drying characteristics of biological materials is a complex phenomenon yet knowledge about drying characteristics is significant to enhance the drying process [20]. Mathematical models are extensively used to understand the drying characteristics/behavior of the product [19]. To describe drying processes, several mathematical models are available in literature. Thin-layer drying can be appropriately explained by thin-layer mathematical drying models for fresh food products such as grapes [21, 22], chili pepper [10, 22–24], stevia leaves [25], and rosemary [9]. Commonly used thin-layer drying models are Newton [9, 26], Midilli and Kucuk [9, 19–21, 23, 27–30], Diffusion approach [9, 14, 31], Page [10, 19, 23, 32–34], Modified Page [23, 25, 35], Two-term [28, 32], Henderson and Pabis [20, 34, 36], Logarithmic [34, 37, 38], Two-term exponential [25, 39], Verma [9, 21, 40], Wang and Singh [25, 28, 34, 41], and Lewis model [20, 42].

However, the limited drying models for dates are found in open literature. Hassan and Hobani [43] studied drying characteristics of two Saudi Arabian dates (Sukkari and Sakie) using laboratory-scale convective dryer at three drying temperatures (70, 80, and 90 °C) and experimental data were evaluated with three thin-layer drying models; among them, Page model provided the good predictions. Kechaou and Maalej [44] investigated moisture diffusivity of single dates by convective dryer under different drying conditions (air temperatures from 30 to 60 °C, relative humidity values from 11.6 to 47.1%, and air velocities from 0.9 to 2.7 m/s) and proposed numerical method to predict moisture movement in a date sample. Falade and Abbo [45] studied hot air-drying pattern of dates with temperature range of 50–80 °C and described moisture transfer with Fick diffusion model. Boubekri, Benmoussa [46] dried dates in a lab-scale indirect solar dryer and used two drying curve equation models to describe the drying characteristics. Chouicha, Boubekri [47] used three types of solar dryers to dry Deglet-Nour dates after being hydrated in distilled water.

İzli [28] studied the drying characteristics of date slices using nine thin-layer drying models and compared with three drying methods: convective (60, 70, and 80 °C), microwave (120 W), and freeze drying. It was reported that among the nine models, Midilli and Kucuk model was the best model for convective and microwave drying, and Two-term model

was the best for freeze drying. Al-Awaadh, Hassan [27] used convective hot air dryer to study drying characteristics of dates at four drying temperature (50 °C, 60 °C, 70 °C, and 80 °C) and three air velocities (0.5, 1.0, and 2.0 m/s). The drying time range was 8.2 to 47.7 h. The experimental data were evaluated with ten thin-layer drying models and the Midilli and Kucuk model was the best fit. Mennouche, Bouchekima [11] and Mennouche, Boubekri [48] used two types of solar dryers to dry the Algerian Deglet-Nour dates.

From the literature review, it is identified that limited studies on drying characteristics of dates at different ripeness stages using solar dryers have been reported. Hence, the present study explores the possibility of using direct sun drying, greenhouse-like solar dryer, and an indirect convective solar dryer for processing fresh dates (khalal, rutab, and tamr). The drying characteristics in three drying approaches were investigated and compared with drying models.

2 Materials and methods

2.1 Date samples

Khalas date that is the premium quality of date cultivar in Oman was selected in this study. Date samples at three ripeness stages (khalal, rutab, and tamr) were harvested from the same tree located at Sultan Qaboos University farm, Muscat (23.59°N and 58.17°E). After harvesting bunches of dates from the tree, date samples were selected in uniform color and size, and free from visible defects in each ripeness stage. The drying process started immediately after harvesting.

2.2 Drying experiments

Fresh date samples were dried in three drying methods such as direct sun drying (DSD), greenhouse-like solar dryer (GSD), and an indirect convective solar dryer (ISD). The

experimental assembly of all three methods was located next to each other to avoid any weather variability. In the DSD, a single layer of dates was placed on perforated trays over a 1-m-high table (Fig. 1(a)). An experimental ISD, having an upper heating compartment and a lower drying compartment, was used (Fig. 1(b)). The heating compartment comprises black granite and a glass cover inclined by 23.6° to the south to receive maximum solar radiation. The dimension length, width, and height of the ISD are 750, 200, and 190 cm, respectively. Forced convection was exerted using 3 small fans withdrawing the ambient air through the heating chamber then the drying chamber with an air velocity of 0.16 m/s. The GSD (Fig. 1(c)) is an airtight 15 × 2-m tunnel, covered with a transparent PE sheet, and divided into two sections: 7.5 × 2-m solar heat collector (air inlet side) and 7.5 × 2-m drying section (fan side). Two fans were fixed opposite to the air inlet side to withdraw the drying air through the cavity of the GSD at a constant air velocity of almost 0.36 m/s.

To monitor temperature and RH of the DSD, one thermocouple (Omega, T type, model: TT-T22S, UK) and one RH sensor (Campbell Scientific Inc., model: HC2S3-L, USA) were fixed near the dryer. Similarly, to measure inlet and outlet air temperature and RH of ISD, four thermocouples (two at the heating compartment and the other two at the drying compartment) and two RH sensors (at the drying compartment) were installed. For GSD, three thermocouples (near to air inlet, middle of the tunnel, and near to fan) and two RH sensors (one at middle and outlet of the tunnel) were fixed. A Campbell Scientific data-logger (CR3000, USA) was used to retrieve data from all sensors at an hourly recording interval. Ambient solar radiation was measured using a pyranometer (Hukseflux Thermal Sensors, model: LP02, sensitivity: 17.87 $\mu\text{V}/(\text{Wm}^{-2})$, the Netherlands).

For the drying experiments, 1 kg of dates in every ripeness stage was uniformly spread (thin layer) on a tray for

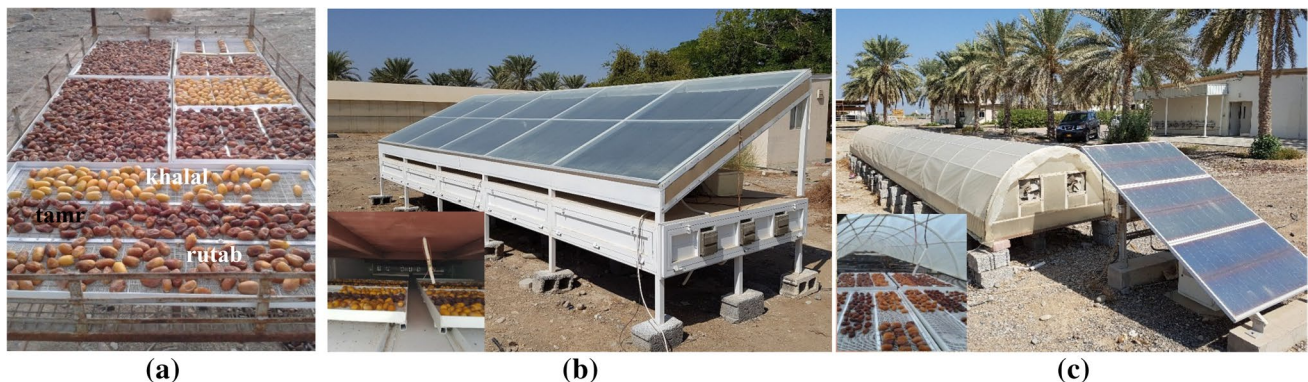


Fig. 1 Photograph of different solar dryer and trays loaded with dates at different ripening stages: **a** direct sun drying, **b** indirect convective solar dryer (inside and outside), and **c** greenhouse-like solar dryer (inside and outside)

each drying technique. A digital weighing scale (A&D Company Ltd., Japan, model: GX4000, capacity: 4100 g, minimum: 0.01 g) was periodically used to measure moisture losses of date samples. In the first 2 h of the experiment, sample weight was taken every 1 h, then in the following 6 h, the weight was taken every 2 h and in the remaining period, the weight was taken every 3 h. The fans were operated daily from 7.00 am (almost 1 h after sunrise) to 6.00 pm (almost 1 h before sunset). Yet, date samples were retained on the dryers and moisture loss/gain during the night was not recorded. Hence, the drying time of dates was considered as 11 h daily and used for computing drying characteristics. Drying was stopped when the moisture content of the dried dates was 35% on dry basis which is considered as a safe level for storage [46].

2.3 Modeling of date drying characteristics

Initial moisture content in wet basis (M_w) and dry basis (M_d) of fresh dates in each ripeness stage was estimated as follows. The moisture content after harvest on wet basis is identified by oven drying at 105 °C until constant weight is reached as follows [23, 49]:

$$M_w = \frac{W_i - W_d}{W_i} \tag{1}$$

$$M_d = \frac{W_i - W_d}{W_d} \tag{2}$$

where W_i and W_d are the initial and oven-dried weight (kg) of the dates, respectively.

The time-changing moisture content (M_t) on dry basis was determined as follows [49]:

$$M_t = \left[\frac{(M_d + 1)W_t}{W_i} - 1 \right] \tag{3}$$

where W_t is the weight of the product at any given time (kg).

The drying rate (DR) in kg/h was estimated using the following equation [19, 20]:

$$DR = -\frac{dM_d}{dt} = -\frac{M_{d,i+1} - M_{d,i}}{T_{i+1} - T_i} = \frac{M_t - M_{t+\Delta T}}{\Delta T} \tag{4}$$

where $M_{d,i}$ is the moisture content at time T_i (simplified as M_i), $M_{d,i+1}$ is the moisture content at time T_{i+1} (simplified as $M_{i+\Delta T}$ at $T+\Delta T$ in kg water/kg dry matter), T is the drying time (h), and ΔT is the drying time difference (h).

The moisture content of date samples at time t was transferred into moisture ratio (MR). The moisture ratio is calculated using Eq. (5) for constant drying air relative humidity [18]:

$$MR = \frac{M_t - M_e}{M_o - M_e} \tag{5}$$

where M_o and M_e are the initial and equilibrium moisture content (kg water/kg dry matter), respectively. During the drying process, the change in solar radiation intensity and drying air temperature ensued continuous fluctuation in relative humidity. Hence, the MR is simplified as follows, owing to the fact that M_e is significantly less than M_o [23]. Therefore, Eq. (5) becomes

$$MR = M_t/M_o \tag{6}$$

The MR values obtained from the experiments are plotted against time and fitted to 11 drying models (thin-layer) (Table 1) in order to find the most appropriate models describing the drying behavior of dates in the three solar

Table 1 Thin-layer drying models applied to describe date drying characteristics in three solar drying methods

| Model no | Model name | Model equation | Reference |
|----------|----------------------|---------------------------------------|-----------|
| 1 | Diffusion approach | $MR = pe^{(-kT)} + (1 - p)e^{(-kpT)}$ | [31] |
| 2 | Henderson and Pabis | $MR = pe^{(-kT)}$ | [36] |
| 2 | Logarithmic | $MR = pe^{(-kT)} + q$ | [37] |
| 4 | Midilli and Kucuk | $MR = pe^{(-kT^n)} + qT$ | [29] |
| 5 | Modified Page | $MR = e^{(-kT^n)}$ | [35] |
| 6 | Newton | $MR = e^{(-kT)}$ | [26] |
| 7 | Page | $MR = e^{(-kT^n)}$ | [33] |
| 8 | Two-term | $MR = pe^{(-k_0T)} + qe^{(-k_1T)}$ | [32] |
| 9 | Two-term exponential | $MR = pe^{(-kT)} + (1 - p)e^{(-kpT)}$ | [39] |
| 10 | Verma | $MR = pe^{(-kT)} + (1 - p)e^{(-gT)}$ | [40] |
| 11 | Wang and Singh | $MR = 1 + pT + qT^2$ | [41] |

MR is the moisture ratio and T is the time (s). k , k_0 , and k_1 are the empirical coefficients (s^{-1}) and p , q , g , and n are the empirical constants

drying methods. SPSS software (version 20.0, USA) was used to find the coefficients of the various models.

The criteria to determine the best-fit between model-predicted and experimental data were the maximum coefficient of determination (R^2), minimum chi-square (χ^2), and minimum root mean square error (RMSE). The following formula were used to calculate these three parameters [18, 23, 25]:

$$R^2 = 1 - \frac{\sum_{i=1}^N (MR_{pre,i} - MR_{exp,i})^2}{\sum_{i=1}^N (\overline{MR}_{pre} - MR_{exp,i})^2} \tag{7}$$

$$\chi^2 = \frac{\sum_{i=1}^N (MR_{exp,i} - MR_{pre,i})^2}{N - m} \tag{8}$$

$$RMSE = \sqrt{\frac{1}{N} \sum_{i=1}^N (MR_{pre,i} - MR_{exp,i})^2} \tag{9}$$

where MR_{exp} is the moisture ratio calculated from the experimental data, MR_{pre} is the moisture ratio predicted from the models, I is any arbitrary observation, N is the total number of observations, and M is the number of model constants.

3 Results and discussion

3.1 Ambient variations

Drying experiments of dates at three ripeness stages in DSD, ISD, and GSD were conducted in the middle of summer

since most of the date cultivars are being harvested in the summer. During the experimental time, solar radiation was ranged from 79 to 948 W/m^2 , while the atmospheric air temperature was in the range of 29 to 50 $^{\circ}C$ and the ambient RH was from 22 to 70% (Figs. 2 and 3). The solar radiation was maximum at midday and minimum at morning. The average diurnal values of 41 $^{\circ}C$, 582 W/m^2 , and 46% were recorded for the ambient air temperature, solar radiation, and RH, respectively. As a result of the high solar intensity and ambient temperature around midday, lower ambient RH was recorded from 11.00 am to 2.00 pm.

Air temperature varied from 29 to 62 $^{\circ}C$ at the inlet of the ISD drying chamber and from 29 to 55 $^{\circ}C$ at the outlet with average diurnal values of 49 and 44 $^{\circ}C$ at the inlet and outlet, respectively (Fig. 4(a) and (b)). In GSD, the drying air temperature varied from 33 to 63 $^{\circ}C$ with an average value of 51 $^{\circ}C$ (Fig. 4(b)). The maximum daily drying air temperature of both ISD and GSD took place at the peak sunshine hour and it was about 10–15 $^{\circ}C$ greater than the ambient temperature. This is attributed to the effective absorption of solar radiation in the heating unit of the ISD and GSD.

Figure 5 presents the variation in RH at the inlet and outlet of the ISD and GSD drying chamber. It was observed that RH exiting the drying chamber of ISD was slightly higher than entering RH. This is due to the moisture release from the dried dates and the drop in air temperature along the drying chamber. However, in the GSD, RH was decreasing along the drying section such that the outlet RH was always lower than that of entering air. This was due to the continuous increase in air temperature throughout the drying section owing to the solar heat gain. The decrease in RH with solar radiation and temperature has been reported

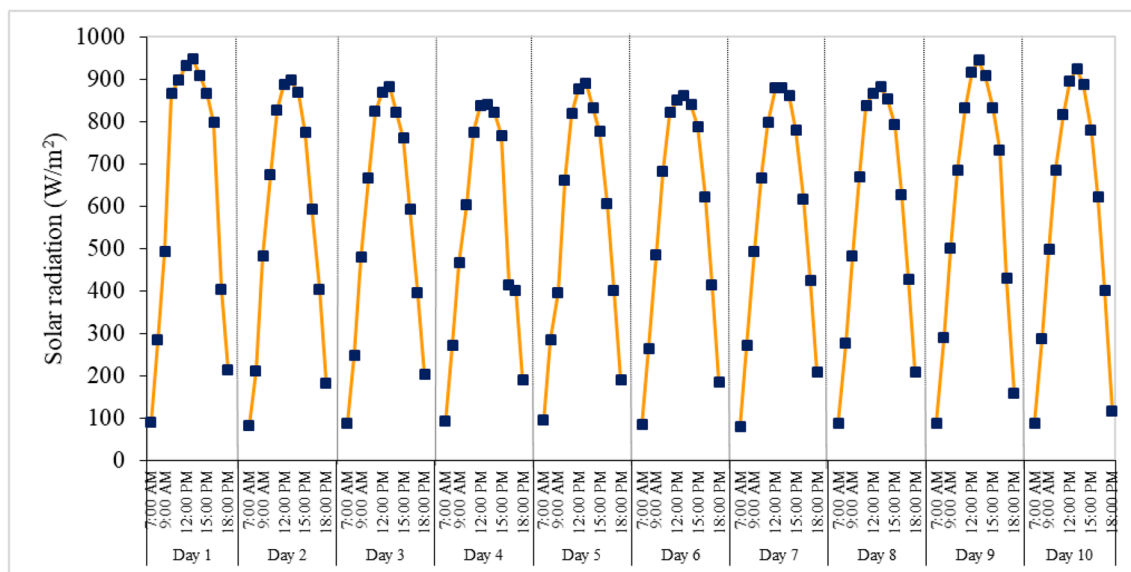


Fig. 2 Solar radiation during the experimental days from July 26 to August 4

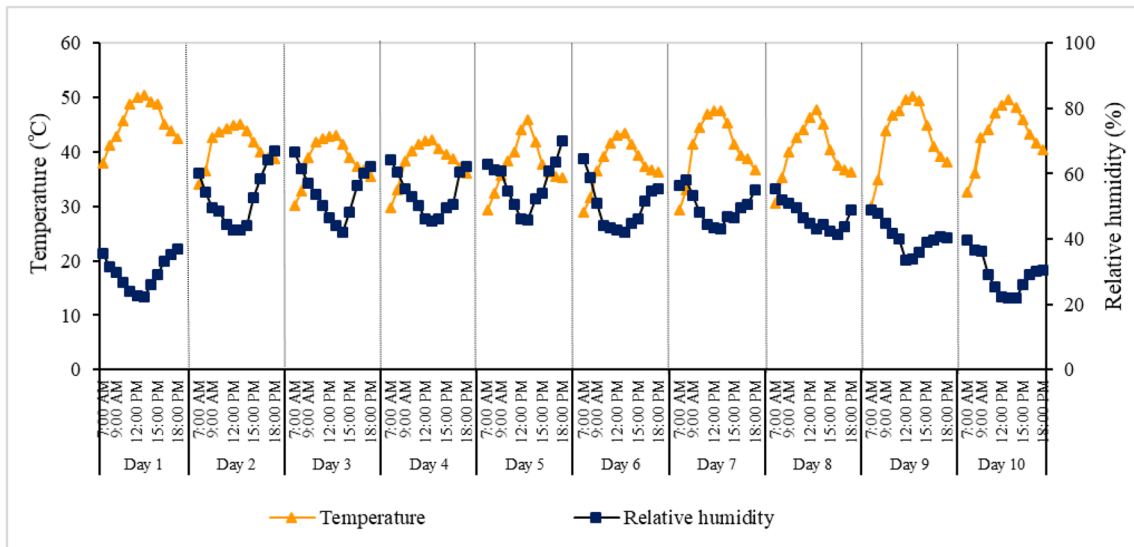


Fig. 3 Ambient temperature and ambient relative humidity during the experimental days from July 26 to August 4

Fig. 4 Variation in temperature at inlet and outlet of ISD and GSD drying sections. **a** Inlet temperature and **b** outlet temperature

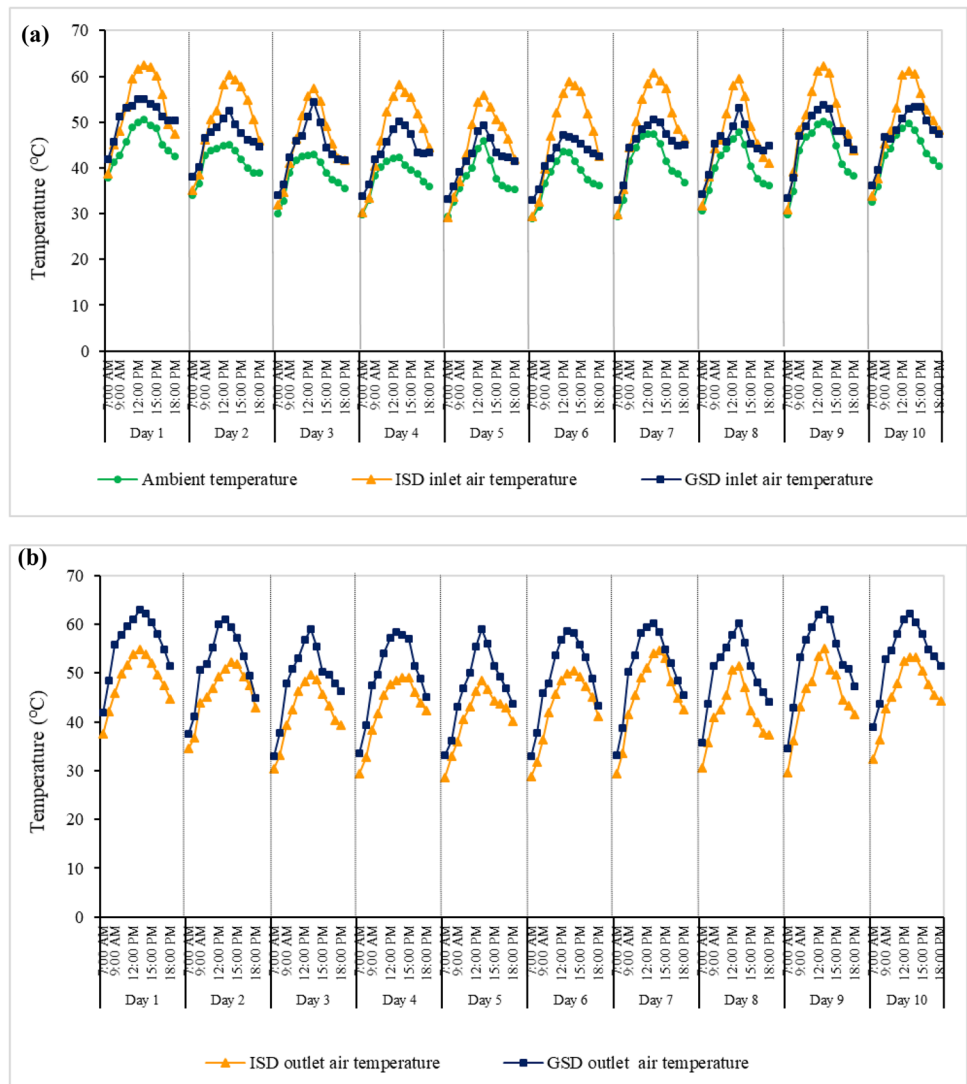
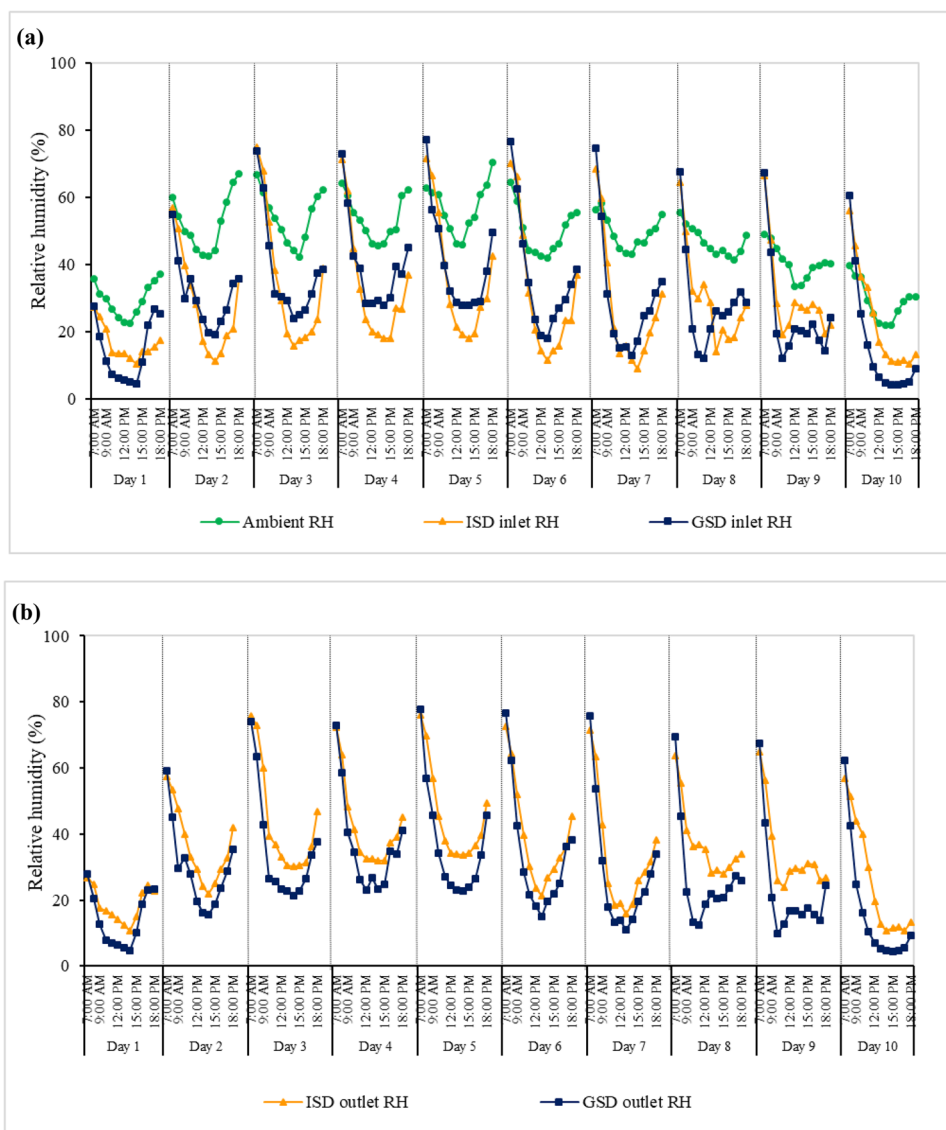


Fig. 5 Variation in relative humidity at inlet and outlet of ISD and GSD drying sections. **a** Inlet RH and **b** outlet RH



by various researchers in drying many agricultural products [14, 22, 23, 50].

In general, RH inside the drying section was always lower than that of ambient air in both dryers (ISD and GSD) during the drying period. This reduced humidity condition enhances the drying rate since low RH increases the air moisture-holding capacity [22]. Hence, GSD and ISD took shorter drying time than DSD as discussed below.

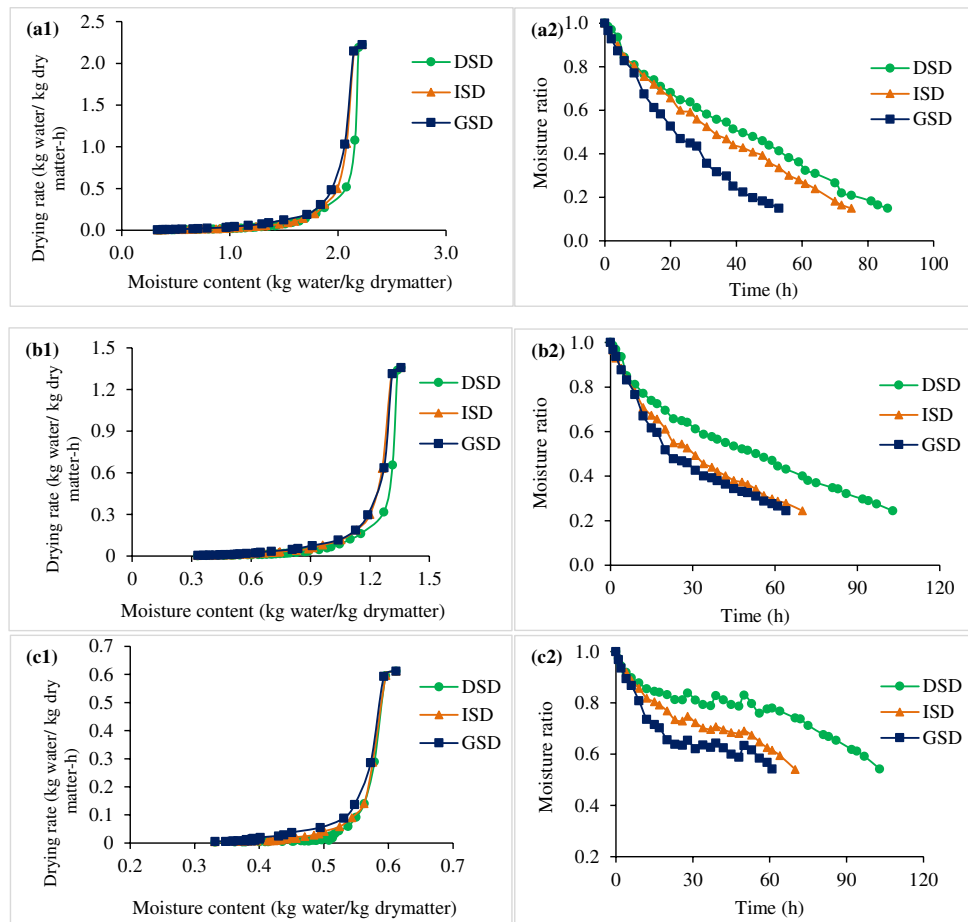
3.2 Drying characteristics

The drying rates of khalal, rutab, and tamr date samples are illustrated in Fig. 6 (a1), (b1), and (c1), respectively. The initial moisture content of 2.23 kg/kg (DB)

for khalal, 1.36 kg/kg (DB) for rutab, and 0.61 kg/kg (DB) for tamr was reduced to 0.33 kg/kg (DB) as a recommended level [45]. A rapid moisture removal (drying rate) was observed at the initial stage (lag phase) then it decreased with time for all ripeness stages. The whole drying course occurred during the falling-rate period, with no constant drying rate period observed.

For DSD, the drying time required to reach to the final moisture content was 86 h for khalal, 103 h for rutab, and 103 h for tamr. However, in ISD the final moisture content was achieved in 75 h for khalal, 70 h for rutab, and 70 h for tamr, and in GSD, it was 53 h, 64, and 61 h, respectively. The DSD took the longest time as a result of the slow drying rate which is attributed to the

Fig. 6 Change in drying rate and moisture ratio of solar-dried dates using DSD, ISD, and GSD at three ripening stages: **a1** and **a2** khalal stage, **b1** and **b2** rutab stage, and **c1** and **c2** tamr stage



lowest average diurnal temperature and humidity (41 °C and 46%, respectively). The higher drying rate in GSD and ISD is due to the elevated temperature and reduced humidity inside the drying sections of both dryers compared with ambient temperature and humidity for DSD. The GSD had higher drying rate than ISD because solar radiation was continuously increasing the temperature inside the drying section, which was not the case in ISD, and because the air velocity in GSD was higher than that in the ISD. Similar results, i.e., higher drying rates with higher air velocity, were reported for apples [51–53] and figs [54].

Figure 6 (a2), (b2), and (c2) depict the moisture ratio with time for khalal, rutab, and tamr, respectively. Throughout the experimental period, moisture ratio was decreasing with time because the moisture transfer within the date samples was mainly governed by the diffusion mechanism [19]. Similar findings were reported in several drying studies of agricultural products such as persimmon slice [19], ghost chili [23], chili pepper [10], and tomato [14].

3.3 Modeling of date drying characteristics

Nonlinear regression was employed to determine the coefficients of the 11 thin-layer drying models, and the results for khalal, rutab, and tamr are summarized in Tables 2, 3, and 4, respectively. The models with R^2 approaching 1, minimum χ^2 , and minimum RMSE represent a best-fit with experimental data.

For khalal dates, Midilli and Kucuk model yielded the maximum R^2 value and the minimum χ^2 and RMSE values for DSD and ISD, whereas Logarithmic model produced the maximum R^2 value and minimum χ^2 and RMSE values for GSD. Two-term model gave the maximum R^2 value and minimum χ^2 and RMSE values for rutab stage in all drying methods. Among all models for tamr dates, Midilli and Kucuk model provided the maximum R^2 value and minimum χ^2 and RMSE values for DSD. Diffusion approach model and Verma model yielded the maximum R^2 value and minimum χ^2 and RMSE values for ISD. Two-term model produced the maximum R^2 value and minimum χ^2 and RMSE values for GSD. Therefore, the above-said models (Midilli and Kucuk,

Table 2 Statistical results of thin-layer drying models for different solar-dried dates at khalal stage

| Drying method | Model no | Model constant | | | | | | RMSE | χ^2 | R^2 | |
|---------------|----------|----------------|------------------------|----------|----------------|----------------|-----------------------|---------|----------------|----------------|-----------------------|
| | | <i>p</i> | <i>q</i> | <i>g</i> | <i>n</i> | <i>k</i> | <i>k</i> ₀ | | | | <i>k</i> ₁ |
| DSD | 1 | 1.00015 | -4.30043 | | | 0.01739 | | | 0.02316 | 0.00059 | 0.9929 |
| | 2 | 0.99155 | | | | 0.01808 | | | 0.03101 | 0.00103 | 0.9848 |
| | 3 | 1.35054 | -0.38702 | | | 0.01050 | | | 0.02356 | 0.00061 | 0.9911 |
| | 4 | 1.01949 | -0.00515 | | 0.54975 | 0.04741 | | | 0.01579 | 0.00028 | 0.9960 |
| | 5 | | | | 1.02153 | 0.01835 | | | 0.03107 | 0.00103 | 0.9848 |
| | 6 | | | | | 0.01829 | | | 0.03122 | 0.00101 | 0.9845 |
| | 7 | | | | 1.02153 | 0.01684 | | | 0.03107 | 0.00103 | 0.9848 |
| | 8 | 0.02372 | 0.98304 | | | | 0.45337 | 0.01787 | 0.03077 | 0.00108 | 0.9851 |
| | 9 | 1.46171 | | | | 0.02163 | | | 0.03022 | 0.00097 | 0.9859 |
| | 10 | 1.00015 | | -0.07480 | | 0.01739 | | | 0.02316 | 0.00059 | 0.9929 |
| | 11 | -0.01515 | 6.431×10^{-5} | | | | | | 0.03103 | 0.00103 | 0.9882 |
| ISD | 1 | 1.00001 | -5.71379 | | | 0.02089 | | | 0.01515 | 0.00026 | 0.9979 |
| | 2 | 0.98629 | | | | 0.02113 | | | 0.02125 | 0.00048 | 0.9930 |
| | 3 | 1.19755 | -0.23164 | | | 0.01467 | | | 0.01508 | 0.00025 | 0.9964 |
| | 4 | 1.00600 | -0.00436 | | 0.66921 | 0.04142 | | | 0.00802 | 0.00007 | 0.9990 |
| | 5 | | | | 1.00431 | 0.02154 | | | 0.02206 | 0.00052 | 0.9926 |
| | 6 | | | | | 0.02153 | | | 0.02207 | 0.00050 | 0.9926 |
| | 7 | | | | 1.00431 | 0.02118 | | | 0.02206 | 0.00052 | 0.9926 |
| | 8 | 0.01754 | 0.98262 | | | | 1.95782 | 0.02102 | 0.02105 | 0.00051 | 0.9931 |
| | 9 | 1.39530 | | | | 0.02445 | | | 0.02153 | 0.00050 | 0.9933 |
| | 10 | 1.00001 | | -0.11938 | | 0.02089 | | | 0.01515 | 0.00026 | 0.9979 |
| | 11 | -0.01821 | 9.728×10^{-5} | | | | | | 0.02539 | 0.00069 | 0.9934 |
| GSD | 1 | 1.03683 | -0.47827 | | | 0.02935 | | | 0.01176 | 0.00016 | 0.9982 |
| | 2 | 1.00832 | | | | 0.03365 | | | 0.01741 | 0.00033 | 0.9962 |
| | 3 | 1.12963 | -0.13712 | | | 0.02642 | | | 0.01143 | 0.00015 | 0.9983 |
| | 4 | 0.99534 | -0.00156 | | 0.98378 | 0.03021 | | | 0.01143 | 0.00016 | 0.9983 |
| | 5 | | | | 1.07089 | 0.03342 | | | 0.01438 | 0.00023 | 0.9974 |
| | 6 | | | | | 0.03330 | | | 0.01779 | 0.00033 | 0.9964 |
| | 7 | | | | 1.07089 | 0.02626 | | | 0.01438 | 0.00023 | 0.9974 |
| | 8 | -0.20163 | 1.19389 | | | | 0.00354 | 0.02551 | 0.01143 | 0.00016 | 0.9983 |
| | 9 | 1.54156 | | | | 0.04114 | | | 0.01332 | 0.00020 | 0.9978 |
| | 10 | 1.03683 | | -0.01404 | | 0.02935 | | | 0.01175 | 0.00016 | 0.9982 |
| | 11 | -0.02789 | | 0.00023 | | | | | 0.01518 | 0.00025 | 0.9976 |

The bold emphasis represents the best-fit model with experimental data

Logarithmic, Diffusion approach, Two-term, and Verma) were considered as the appropriate models to describe the drying process of Khalas dates at khalal, rutab, and tamr stages in the corresponding drying techniques. These models are expressed as follows:

For khalal stage

$$DSD : MR = 1.01949 \exp(-0.04741T^{0.54975}) - 0.00515 T \tag{10}$$

$$ISD : MR = 1.00600 \exp(-0.04142T^{0.66921}) - 0.00436 T \tag{11}$$

$$GSD : MR = 1.12963 \exp(-0.02642T) - 0.13712 \tag{12}$$

For rutab stage

$$DSD : MR = 0.14212 \exp(-0.18042T) + 0.87529 \exp(-0.01134 T) \tag{13}$$

$$ISD : MR = 0.17373 \exp(-0.10796T) + 0.82346 \exp(-0.01709 T) \tag{14}$$

$$GSD : MR = 0.52053 \exp(-0.06372 T) + 0.48950 \exp(-0.01031 T) \tag{15}$$

Table 3 Statistical results of thin-layer drying models for different solar-dried dates at rutab stage

| Drying method | Model no | Model constant | | | | | | RMSE | χ^2 | R^2 | |
|---------------|----------|----------------|------------------------|---------|---------|---------|----------------|----------------|----------------|----------------|---------------|
| | | p | q | g | n | k | k_0 | | | | k_1 |
| DSD | 1 | 0.12544 | 0.07181 | | | 0.15785 | | | 0.01349 | 0.00020 | 0.9961 |
| | 2 | 0.94315 | | | | 0.01276 | | | 0.02633 | 0.00073 | 0.9844 |
| | 3 | 0.82045 | 0.14124 | | | 0.01721 | | | 0.02383 | 0.00062 | 0.9872 |
| | 4 | 1.02569 | -0.00171 | | 0.59232 | 0.05531 | | | 0.01356 | 0.00021 | 0.9959 |
| | 5 | | | | 0.79552 | 0.01309 | | | 0.01784 | 0.00034 | 0.9928 |
| | 6 | | | | | 0.01400 | | | 0.03628 | 0.00135 | 0.9858 |
| | 7 | | | | 0.79552 | 0.03177 | | | 0.01784 | 0.00034 | 0.9928 |
| | 8 | 0.14212 | 0.87529 | | | | 0.18042 | 0.01134 | 0.01287 | 0.00019 | 0.9963 |
| | 9 | 0.11283 | | | | 0.10397 | | | 0.01701 | 0.00031 | 0.9942 |
| | 10 | 0.12544 | | 0.01134 | | 0.15785 | | | 0.01349 | 0.00020 | 0.9961 |
| | 11 | -0.01374 | 6.772×10^{-5} | | | | | | 0.03771 | 0.00151 | 0.9780 |
| ISD | 1 | 0.17201 | 0.15151 | | | 0.11341 | | | 0.00718 | 0.00006 | 0.9990 |
| | 2 | 0.95287 | | | | 0.02064 | | | 0.02107 | 0.00048 | 0.9915 |
| | 3 | 0.81110 | 0.16837 | | | 0.03037 | | | 0.01144 | 0.00015 | 0.9974 |
| | 4 | 1.00551 | 8.520×10^{-6} | | 0.80986 | 0.04449 | | | 0.00754 | 0.00007 | 0.9989 |
| | 5 | | | | 0.81890 | 0.02126 | | | 0.00769 | 0.00006 | 0.9989 |
| | 6 | | | | | 0.02215 | | | 0.02951 | 0.00090 | 0.9933 |
| | 7 | | | | 0.81890 | 0.04269 | | | 0.00769 | 0.00006 | 0.9989 |
| | 8 | 0.17373 | 0.82346 | | | | 0.10796 | 0.01709 | 0.00714 | 0.00006 | 0.9990 |
| | 9 | 0.15736 | | | | 0.11220 | | | 0.00774 | 0.00006 | 0.9990 |
| | 10 | 0.17201 | | 0.01718 | | 0.11341 | | | 0.00718 | 0.00006 | 0.9990 |
| | 11 | -0.02186 | 1.688×10^{-4} | | | | | | 0.02678 | 0.00077 | 0.9910 |
| GSD | 1 | 0.55320 | 0.15704 | | | 0.05812 | | | 0.01240 | 0.00017 | 0.9973 |
| | 2 | 0.94804 | | | | 0.02384 | | | 0.03731 | 0.00151 | 0.9755 |
| | 3 | 0.77413 | 0.22794 | | | 0.04449 | | | 0.01353 | 0.00021 | 0.9967 |
| | 4 | 1.01250 | 0.00199 | | 0.90038 | 0.04634 | | | 0.01435 | 0.00024 | 0.9962 |
| | 5 | | | | 0.77816 | 0.02479 | | | 0.02111 | 0.00048 | 0.9922 |
| | 6 | | | | | 0.02571 | | | 0.04344 | 0.00196 | 0.9794 |
| | 7 | | | | 0.77816 | 0.05629 | | | 0.02111 | 0.00048 | 0.9922 |
| | 8 | 0.52053 | 0.48950 | | | | 0.06372 | 0.01031 | 0.01199 | 0.00017 | 0.9974 |
| | 9 | 0.20162 | | | | 0.09783 | | | 0.02170 | 0.00051 | 0.9923 |
| | 10 | 0.55321 | | 0.00913 | | 0.05812 | | | 0.01240 | 0.00017 | 0.9973 |
| | 11 | -0.02620 | 2.402×10^{-4} | | | | | | 0.03139 | 0.00107 | 0.9853 |

The bold emphasis represents the best-fit model with experimental data

For tamr stage

$$\text{DSD : } MR = 1.00096 \exp(-0.06811 T^{0.07521}) - 0.00289 T \tag{16}$$

$$\text{ISD : (i) } MR = 0.85651 \exp(-0.00532T) + 0.14349 \exp(-0.16592 T) \tag{17}$$

$$\text{(ii) } MR = 0.14350 \exp(-0.16583 T) + 0.85650 \exp(-0.00532 T) \tag{18}$$

$$\text{GSD : } MR = 0.66459 \exp(-0.00224 T) + 0.34291 \exp(-0.10094 T) \tag{19}$$

Al-Awaadh et al. [27] found that the drying process of Sukkari dates was best described by the Midilli and Kucuk model. İzli [28] reported that Midilli and Kucuk and Two-term models were found as the good fit in representing the drying of date slices in microwave, convective, and freeze-drying methods. The study found that the Logarithmic model was suitable for describing the thin-layer drying of pepper [38], while the Diffusion approach model was suitable for describing the thin-layer drying of tomato [14]. Verma model was identified to be the best-fit model to describe the drying process of peaches in direct sun drying [37].

Table 4 Statistical results of thin-layer drying models for different solar-dried dates at tamr stage

| Drying method | Model no | Model constant | | | | | | RMSE | χ^2 | R^2 | |
|---------------|-----------|----------------|------------------------|----------------|----------------|----------------|----------------|----------------|----------------|----------------|---------------|
| | | p | Q | g | n | k | k_0 | | | | k_1 |
| DSD | 1 | 0.92073 | 127.65758 | | | 0.00373 | | | 0.03052 | 0.00102 | 0.9114 |
| | 2 | 0.93897 | | | | 0.00405 | | | 0.03366 | 0.00120 | 0.8921 |
| | 3 | -0.24292 | 1.15669 | | | -0.00849 | | | 0.03048 | 0.00101 | 0.9115 |
| | 4 | 1.00096 | -0.00289 | | 0.07521 | 0.06811 | | | 0.03005 | 0.00102 | 0.9171 |
| | 5 | | | | 0.64944 | 0.00280 | | | 0.03673 | 0.00143 | 0.8743 |
| | 6 | | | | | 0.00510 | | | 0.04592 | 0.00217 | 0.8889 |
| | 7 | | | | 0.64944 | 0.02199 | | | 0.03673 | 0.00143 | 0.8743 |
| | 8 | 0.92074 | 0.08267 | | | | 0.00373 | 0.49398 | 0.03052 | 0.00105 | 0.9114 |
| | 9 | 0.04372 | | | | 0.10083 | | | 0.03868 | 0.00158 | 0.8943 |
| | 10 | 0.07927 | | 0.00373 | | 0.47642 | | | 0.03052 | 0.00102 | 0.9114 |
| | 11 | -0.00551 | 1.705×10^{-5} | | | | | | 0.04566 | 0.00221 | 0.8707 |
| ISD | 1 | 0.85651 | 31.18856 | | | 0.00532 | | | 0.01629 | 0.00030 | 0.9801 |
| | 2 | 0.92966 | | | | 0.00716 | | | 0.03039 | 0.00010 | 0.9307 |
| | 3 | 0.40369 | 0.56458 | | | 0.03101 | | | 0.02324 | 0.00061 | 0.9594 |
| | 4 | 1.01052 | -0.00080 | | 0.50234 | 0.05266 | | | 0.01816 | 0.00039 | 0.9752 |
| | 5 | 0.00465 | | | 0.58683 | | | | 0.01842 | 0.00037 | 0.9746 |
| | 6 | | | | | 0.00897 | | | 0.04651 | 0.00225 | 0.9351 |
| | 7 | | | | 0.58683 | 0.04279 | | | 0.01842 | 0.00037 | 0.9746 |
| | 8 | 0.85643 | 0.14320 | | | | 0.00532 | 0.16519 | 0.01629 | 0.00031 | 0.9801 |
| | 9 | 0.07822 | | | | 0.09220 | | | 0.03187 | 0.00110 | 0.9605 |
| | 10 | 0.14350 | | 0.00532 | | 0.16583 | | | 0.01629 | 0.00030 | 0.9801 |
| | 11 | -0.01180 | 9.142×10^{-5} | | | | | | 0.03457 | 0.00129 | 0.9380 |
| GSD | 1 | 0.65919 | 45.70750 | | | 0.00211 | | | 0.01828 | 0.00038 | 0.9805 |
| | 2 | 0.89420 | | | | 0.00908 | | | 0.05492 | 0.00328 | 0.8224 |
| | 3 | 0.41154 | 0.58916 | | | 0.07643 | | | 0.01937 | 0.00043 | 0.9778 |
| | 4 | 1.01707 | 0.00469 | | 0.72727 | 0.06072 | | | 0.02209 | 0.00058 | 0.9712 |
| | 5 | | | | 0.49170 | 0.00569 | | | 0.03073 | 0.00103 | 0.9455 |
| | 6 | | | | | 0.01225 | | | 0.07544 | 0.00593 | 0.8384 |
| | 7 | | | | 0.49170 | 0.07874 | | | 0.03073 | 0.00103 | 0.9455 |
| | 8 | 0.66459 | 0.34291 | | | | 0.00224 | 0.10094 | 0.01814 | 0.00039 | 0.9806 |
| | 9 | 0.10367 | | | | 0.09360 | | | 0.05715 | 0.00355 | 0.8884 |
| | 10 | 0.34080 | | 0.00211 | | 0.09626 | | | 0.01827 | 0.00038 | 0.9804 |
| | 11 | -0.01873 | 2.061×10^{-4} | | | | | | 0.04005 | 0.00174 | 0.9286 |

The bold emphasis represents the best-fit model with experimental data

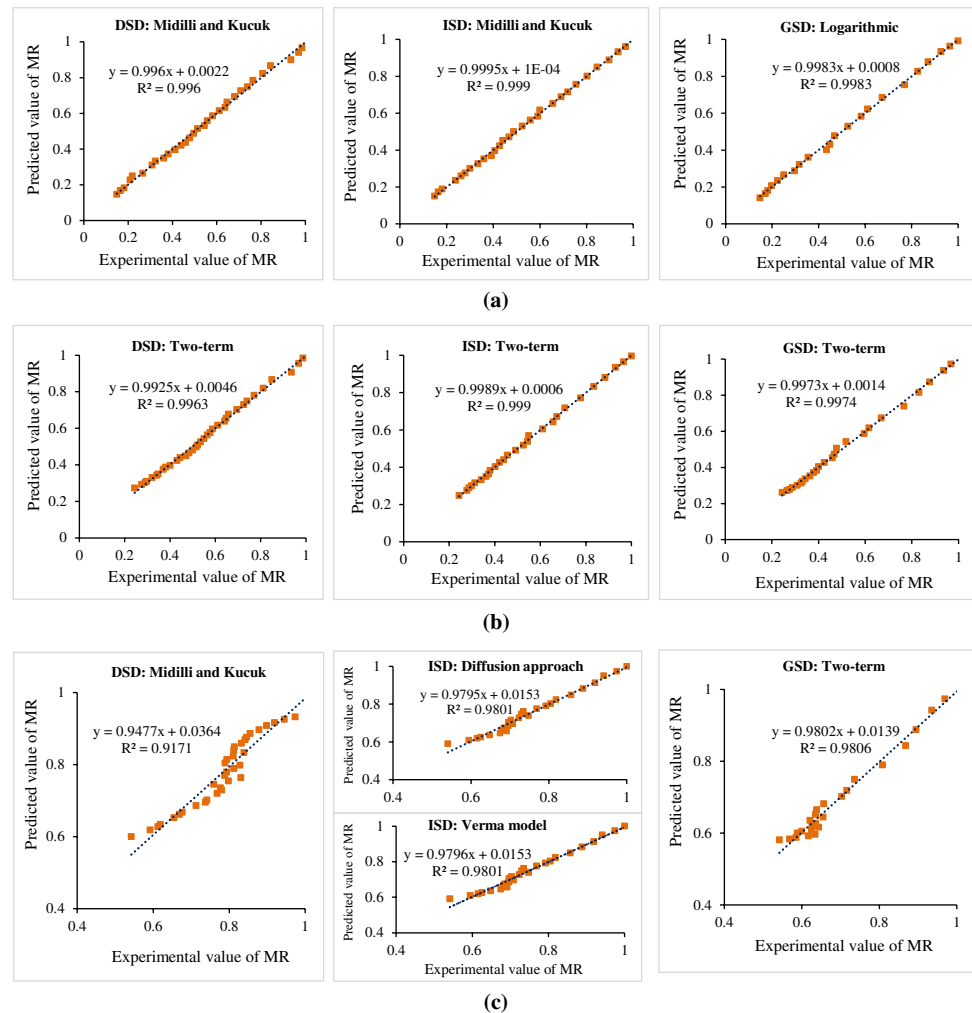
3.4 Validation with experimental data

To validate the suitability of the selected models for each respective ripeness stage and drying method, the predicted moisture ratio from these models was plotted against the experimental data, as shown in Fig. 7. Based on visual analysis and R^2 values near 1, it can be concluded that the selected models accurately predicted the moisture ratio. From visual observations and R^2 values close to 1, it be clearly observed that the selected models were accurately predicting the moisture ratio.

4 Conclusion

The drying experiments were carried out to examine the drying behavior of fresh dates at three ripening stages (khalal, rutab, and tamr) using three drying methods: direct sun drying, greenhouse-like solar dryer, and an indirect convective solar dryer. The experimental data were fitted with 11 thin-layer drying models to describe the drying process. The maximum solar radiation (948 W/m^2) and ambient air temperature ($50 \text{ }^\circ\text{C}$) were recorded at midday. Due to higher solar intensity and ambient temperature, the ambient RH

Fig. 7 Comparison of the experimental and predicted value of moisture ratio of solar-dried dates using DSD, ISD, and GSD at different ripening stage: **a** khalal stage, **b** rutab stage, and **c** tamr stage



was lower in midday, which enhances the drying rate at mid-day. For both ISD and GSD, the maximum daily drying air temperature was about 10–15 °C higher than the ambient temperature, which offered shorter drying time of 70–75 h for ISD and 53–64 h for GSD to achieve the desired moisture content of 35% on dry basis. The direct sun drying method took the longest drying time (86 to 103 h) for all three ripeness stages. The results of fitting showed that the Midilli and Kucuk, Logarithmic, Two-term, Diffusion approach, and Verma models had a higher coefficient of determination and lower reduced chi-square and root mean square error values. Therefore, these models are deemed the most suitable for representing the thin-layer drying process of Khalas dates at the respective stage of ripeness and drying method. Furthermore, dryer performance, economic feasibility, and energy and exergy analyses should be carried out as future studies to use these dryers for other agricultural products.

Acknowledgements First author would like to express their sincere gratitude to the administration of Sultan Qaboos University, Muscat for the providing of Khalas date samples used in this study.

Author contribution T. Seerangurayar — conceptualization (lead), methodology (lead), investigation (lead), original draft (lead), review and editing (lead); Abdulrahim M. Al-Ismaili — conceptualization (lead), methodology (lead), investigation (lead), resources, original draft (lead); L. H. Janitha Jeewantha — methodology (supporting), investigation (lead); G. Jeevarathinam — conceptualization (supporting), methodology (supporting), review and editing (lead); R. Pandiselvam — methodology (supporting), resources, data analysis, review and editing (supporting); S. Dinesh Kumar: methodology (supporting), review and editing (supporting); M. Mohanraj and Punit Singh — methodology (supporting), review and editing (supporting).

Data availability All data are available upon request.

Declarations

Ethics approval Not applicable.

Consent for publication All authors agreed on the publication of this research work.

Competing interests The authors declare no competing interests.

References

- Vayalil PK (2012) Date fruits (*Phoenix dactylifera* Linn): an emerging medicinal food. *Crit Rev Food Sci Nutr* 52(3):249–271
- MAF (2015) Agricultural and fisheries production and economics in 2011–14; Directorate general of planning and development, ministry of agriculture and fisheries (MAF), Sultanate of Oman, 2015
- FAOSTAT (2017) FAO Statistics. <http://www.fao.org/faostat/en/#data/QC>. Accessed November 2017
- Chong CH, Law CL, Cloke M et al (2009) Drying models and quality analysis of sun-dried ciku. *Drying Technol* 27(9):985–992
- Seerangurayar T, Manickavasagan A, Al-Ismaili AM, Al-Mulla YA (2017) Effect of carrier agents on flowability and microstructural properties of foam-mat freeze dried date powder. *J Food Eng* 215:33–43
- Ashraf Z, Hamidi-Esfahani Z (2011) Date and date processing: a review. *Food Rev Intl* 27(2):101–133
- Al-Farsi MA, Lee CY (2008) Nutritional and functional properties of dates: a review. *Crit Rev Food Sci Nutr* 48(10):877–887
- Fudholi A, Sopian K, Alghoul M et al (2015) Performances and improvement potential of solar drying system for palm oil fronds. *Renew Energy* 78:561–565
- Mghazli S, Ouhammou M, Hidar N et al (2017) Drying characteristics and kinetics solar drying of Moroccan rosemary leaves. *Renew Energy* 108:303–310
- Tunde-Akintunde T (2011) Mathematical modeling of sun and solar drying of chilli pepper. *Renew Energy* 36(8):2139–2145
- Mennouche D, Bouchekima B, Boubekri A et al (2014) Valorization of rehydrated Deglet-Nour dates by an experimental investigation of solar drying processing method. *Energy Convers Manage* 84:481–487
- Fadhel A, Kooli S, Farhat A, Bellghith A (2005) Study of the solar drying of grapes by three different processes. *Desalination* 185(1–3):535–541
- Fudholi A, Sopian K, Yazdi MH et al (2014) Performance analysis of solar drying system for red chili. *Sol Energy* 99:47–54
- Sacilik K, Keskin R, Elicin AK (2006) Mathematical modelling of solar tunnel drying of thin layer organic tomato. *J Food Eng* 73(3):231–238
- El-Beltagy A, Gamea G, Essa AA (2007) Solar drying characteristics of strawberry. *J Food Eng* 78(2):456–464
- Goyal R, Kingsly A, Manikantan M, Ilyas S (2007) Mathematical modelling of thin layer drying kinetics of plum in a tunnel dryer. *J Food Eng* 79(1):176–180
- Karthikeyan A, Murugavel S (2018) Thin layer drying kinetics and exergy analysis of turmeric (*Curcuma longa*) in a mixed mode forced convection solar tunnel dryer. *Renew Energy* 128:305–312
- Lakshmi D, Muthukumar P, Layek A, Nayak PK (2018) Drying kinetics and quality analysis of black turmeric (*Curcuma caesia*) drying in a mixed mode forced convection solar dryer integrated with thermal energy storage. *Renew Energy* 120:23–34
- Doymaz İ (2012) Evaluation of some thin-layer drying models of persimmon slices (*Diospyros kaki* L.). *Energy Convers Manage* 56:199–205
- Shi Q, Zheng Y, Zhao Y (2013) Mathematical modeling on thin-layer heat pump drying of yacon (*Smallanthus sonchifolius*) slices. *Energy Convers Manage* 71:208–216
- Doymaz İ (2012) Sun drying of seedless and seeded grapes. *J Food Sci Technol* 49(2):214–220
- ELKhadraoui A, Kooli S, Hamdi I, Farhat A (2015) Experimental investigation and economic evaluation of a new mixed-mode solar greenhouse dryer for drying of red pepper and grape. *Renew Energy* 77:1–8
- Rabha D, Muthukumar P, Somayaji C (2017) Experimental investigation of thin layer drying kinetics of ghost chilli pepper (*Capiscum chinense* Jacq.) dried in a forced convection solar tunnel dryer. *Renew Energy* 105:583–589
- Fudholi A, Othman MY, Ruslan MH, Sopian K (2013) Drying of Malaysian *Capiscum annum* L. (red chili) dried by open and solar drying. *Int J Photoenergy*. <https://doi.org/10.1155/2013/167895>
- Téllez MC, Figueroa IP, Téllez BC et al (2018) Solar drying of Stevia (*Rebaudiana Bertoni*) leaves using direct and indirect technologies. *Solar Energy* 159:898–907
- Ayensu A (1997) Dehydration of food crops using a solar dryer with convective heat flow. *Sol Energy* 59(4–6):121–126
- Al-Awaadh AM, Hassan BH, Ahmed KM (2015) Hot air drying characteristics of Sukkari date (*Phoenix dactylifera* L.) and effects of drying condition on fruit color and texture. *Int J Food Eng* 11(3):421–434
- İzli G (2016) Total phenolics, antioxidant capacity, colour and drying characteristics of date fruit dried with different methods. *Food Sci Technol* 37:139–147
- Midilli A, Kucuk H, Yapar Z (2002) A new model for single-layer drying. *Drying Technol* 20(7):1503–1513
- Essalhi H, Benchrifa M, Tadili R, Bargach M (2018) Experimental and theoretical analysis of drying grapes under an indirect solar dryer and in open sun. *Innov Food Sci Emerg Technol* 49:58–64
- Akpinar E, Midilli A, Bicer Y (2003) Single layer drying behaviour of potato slices in a convective cyclone dryer and mathematical modeling. *Energy Convers Manage* 44(10):1689–1705
- Henderson S (1974) Progress in developing the thin layer drying equation. *Trans ASAE* 17(6):1167–1168
- Diamante LM, Munro PA (1993) Mathematical modelling of the thin layer solar drying of sweet potato slices. *Sol Energy* 51(4):271–276
- Gulcimen F, Karakaya H, Durmus A (2016) Drying of sweet basil with solar air collectors. *Renew Energy* 93:77–86
- Panchariya P, Popovic D, Sharma A (2002) Thin-layer modelling of black tea drying process. *J Food Eng* 52(4):349–357
- Chavan B, Yakupitiyage A, Kumar S (2008) Mathematical modeling of drying characteristics of Indian mackerel (*Rastrilliger kangurta*) in solar-biomass hybrid cabinet dryer. *Drying Technol* 26(12):1552–1562
- Toğrul İT, Pehlivan D (2004) Modelling of thin layer drying kinetics of some fruits under open-air sun drying process. *J Food Eng* 65(3):413–425
- Vengaiiah P, Pandey J (2007) Dehydration kinetics of sweet pepper (*Capiscum annum* L.). *J Food Eng* 81(2):282–286
- Erbay Z, Icier F (2010) A review of thin layer drying of foods: theory, modeling, and experimental results. *Crit Rev Food Sci Nutr* 50(5):441–464
- Verma LR, Bucklin R, Endan J, Wratten F (1985) Effects of drying air parameters on rice drying models. *Trans ASAE* 28(1):296–0301
- Wang C, Singh R (1978) A single layer drying equation for rough rice. *ASAE paper* 78–3001:33
- Sansaniwal SK, Kumar M, Sahdev RK et al (2022) Toward natural convection solar drying of date palm fruits (*Phoenix dactylifera* L.): an experimental study. *Environ Progress Sustain Energy* 41(6):e13862
- Hassan BH, Hobani AI (2000) Thin-layer drying of dates. *J Food Process Eng* 23(3):177–189

44. Kechaou N, Maalej M (2000) A simplified model for determination of moisture diffusivity of date from experimental drying curves. *Drying Technol* 18(4–5):1109–1125
45. Falade KO, Abbo ES (2007) Air-drying and rehydration characteristics of date palm (*Phoenix dactylifera* L.) fruits. *J Food Eng* 79(2):724–730
46. Boubekri A, Benmoussa H, Mennouche D (2009) Solar drying kinetics of date palm fruits assuming a step-wise air temperature change. *J Eng Sci Technol* 4(3):292–304
47. Chouicha S, Boubekri A, Mennouche D et al (2014) Valorization study of treated deglet-nour dates by solar drying using three different solar driers. *Energy Procedia* 50:907–916
48. Mennouche D, Boubekri A, Chouicha S et al (2017) Solar drying process to obtain high standard “Deglet-Nour” date fruit. *J Food Process Eng* 40(5):e12546
49. El-Sebaï A, Shalaby S (2013) Experimental investigation of an indirect-mode forced convection solar dryer for drying thymus and mint. *Energy Convers Manage* 74:109–116
50. Rajkumar P, Kulanthaisami S, Raghavan G et al (2007) Drying kinetics of tomato slices in vacuum assisted solar and open sun drying methods. *Drying Technol* 25(7–8):1349–1357
51. Vega-Gálvez A, Ah-Hen K, Chacana M et al (2012) Effect of temperature and air velocity on drying kinetics, antioxidant capacity, total phenolic content, colour, texture and microstructure of apple (var. Granny Smith) slices. *Food Chem* 132(1):51–59
52. Velić D, Planinić M, Tomas S, Bilić M (2004) Influence of air-flow velocity on kinetics of convection apple drying. *J Food Eng* 64(1):97–102
53. Kaya A, Aydın O, Demirtaş C (2007) Drying kinetics of red delicious apple. *Biosys Eng* 96(4):517–524
54. Babalis SJ, Belessiotis VG (2004) Influence of the drying conditions on the drying constants and moisture diffusivity during the thin-layer drying of figs. *J Food Eng* 65(3):449–458

Publisher's note Springer Nature remains neutral with regard to jurisdictional claims in published maps and institutional affiliations.

Springer Nature or its licensor (e.g. a society or other partner) holds exclusive rights to this article under a publishing agreement with the author(s) or other rightsholder(s); author self-archiving of the accepted manuscript version of this article is solely governed by the terms of such publishing agreement and applicable law.